13th International Conference on
Structural Health Monitoring of Intelligent Infrastructure
DOI: 10.3217/978-3-99161-057-1-176

# Study on Methods for Identifying and Evaluating Damage to Cross-Sea Bridges Subjected to Ship Collisions

Jian Guo[1], Yuhao Cui[2], Zheng Wang[2], Jiahui Wu[2]
[1]State Key Laboratory of Bridge Intelligent and Green Construction, Southwest Jiaotong University, Chengdu, Sichuan 610000, China
[2]School of Civil Engineering, Southwest Jiaotong University, Chengdu, Sichuan 610000, China
email: guoj@swjtu.edu.cn, cuiyuhao@my.swjtu.edu.cn, wzheng@my.swjtu.edu.cn, wujiahui@my.swjtu.edu.cn

ABSTRACT: Cross-sea bridges are crucial transportation links, ensuring smooth maritime traffic and protecting public safety and property. However, ship collisions pose a serious threat, potentially causing extensive damage to bridges, disrupting traffic, polluting the environment, and leading to casualties. Therefore, it is extremely important to develop methods for identifying and evaluating damage to cross-sea bridges caused by ship collisions. A study has been conducted utilizing a combined approach of numerical simulation and experimental validation to analyze the structural dynamic responses of bridges subjected to ship collisions. Based on the insights gained, a structural damage assessment method combining response surface method and Monte Carlo simulation has been introduced. This method takes into account factors such as the impact height and kinetic energy during ship-bridge collisions, establishing a comprehensive evaluation index system. This approach offers a holistic view of the damage state of bridges subjected to ship collisions, providing a scientific foundation for subsequent emergency response and repair strategies. Ultimately, the research aims to mitigate the adverse effects of ship collisions on the structural integrity of cross-sea bridges.

KEY WORDS: Ship-bridge Collisions; Damage Assessment; Impact Test; Response Surface Method.

## 1 INTRODUCTION

Currently, the safety issues related to bridge ship collisions have garnered widespread attention. However, relevant research primarily focuses on impact force estimation and studies on bridge anti-collision facilities (Chen et al., 2022; Nian et al., 2016). However, previous studies have struggled to capture the damage evolution characteristics of bridges under varying ship kinetic energy impacts. Conducting fragility analysis for bridge ship collisions can predict the probability of structural damage at various levels, providing practical engineering value for structural design, reinforcement, and maintenance decision-making.

The seismic fragility analysis of bridges has garnered extensive attention from scholars both domestically and internationally. Song et al. (2024) conducted a comprehensive brittleness assessment of specimen viaducts under various ground motion excitation schemes in order to evaluate the impact of modeling detail and analysis complexity on estimating seismic performance. Wang et al. (2025) established an analysis model of the degradation state of a large cantilever cap bridge, and studied the seismic vulnerability of the bridge structure under different service times based on the OpenSees platform. Li et al. (2025) proposed a copula-based approach proposed for seismic vulnerability analysis by incorporating the uncertainty of scour depth into the assessment of bridge seismic performance. However, research on the fragility of bridges under ship collisions is very limited. Kameshwar et al. (2018) developed a meta-model to estimate the force requirements and vulnerability of bridge pillars under barge impact. Fu et al. (2024) proposed a new brittleness assessment framework based on the residual bearing capacity of piers. Zhong et al. (2024) propose a fragility based framework to determine the most unfavorable position of a bridge column for collision with a barge.

However, there is currently no widely accepted and convincing damage indicator for assessing pier damage under ship collisions. Fan et al. (2021) proposed a bridge ship collision vulnerability analysis method combining a simplified finite element model with a response surface agent model, and obtained the bridge vulnerability curves under two types of typical ship impacts. In recent years, some scholars have also applied the response surface method to the parameter analysis and reliability analysis of bridges under impact, significantly improving computational efficiency. Fan et al. (2018) conducted an extensive parametric study using the response surface method to investigate the effects of reinforcement ratio, UHPFRC sheath thickness, UHPFRC strength, and initial impact velocity. Duan et al. (2024) proposed an efficient hybrid response surface method to study the system reliability of pile-reinforced slopes.

In this study, the stress-strain behavior at the base of the pier under ship impact was investigated through a combined experimental and finite element comparative analysis. Based on the response surface, a new bridge impact damage index is proposed and applied to bridge brittleness assessment. By establishing a full-scale finite element model of the bridge, a multi-factor ship collision simulation analysis was conducted. Fragility curves of the pier under different influencing factors were obtained, providing a reference for the fragility analysis of bridges subjected to ship collisions.

## 2 EXPERIMENTAL OVERVIEW

The non-navigational spans of the prototype bridge are 60-meter span continuous concrete girder bridges, with the main body of the bridge constructed using marine-grade concrete

DOI: 10.3217/978-3-99161-057-1-176

C40. Based on the scale ratio, the overall schematic diagram of the bridge model structure, as shown in the Figure 1, was established by fully considering the interaction relationships between the pile caps, pile foundations, bearings, and girder segments. Hollow circular steel pipes with a diameter of 89 mm and a wall thickness of 2.5 mm were used to simulate the pile foundations. The pile length was determined to be 75 cm using the 8-times equivalent pile diameter method, and the piles were embedded into the pile cap to a depth of 5 cm.

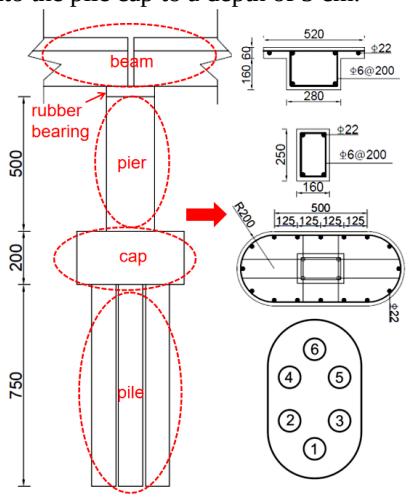


Figure 1. The dimensional drawing of the scaled full-bridge model (mm).

To simplify the design, the ship model consists of a bow model and a stern model, connected by a force sensor in between. Since the stern model does not directly contact the bridge model during the collision process, it is primarily responsible for accommodating sand and stone ballast to achieve different mass conditions. The bow model mainly comprises an internal structure and an external shell structure. The external shell structure is constructed by assembling 1 mm steel plates. Given the difficulty in replicating every detail of the actual bow's internal structure, the internal structure of the bow is composed of two equivalent supports, which are fabricated by welding steel bars with a diameter of 6 mm.

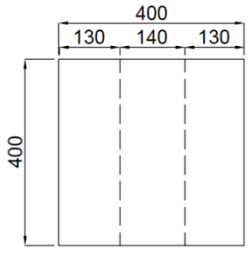


(a) Top view

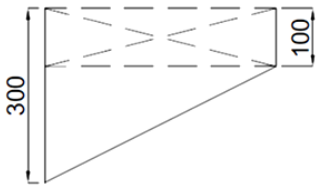


(b) Side view

Figure 2. The dimensional specifications of the scaled bow model (mm).

Considering the test site conditions, a pendulum-type loading device powered by gravitational acceleration was employed. The frame of the loading device was constructed by welding I-beams, and its base was securely anchored to the ground trough using anchor bolts. A movable beam was installed at the top of the frame, equipped with universal wheels. The ship model was suspended at a pre-calculated height and released by a triggering mechanism. Utilizing gravitational acceleration, the ship model attained a certain horizontal velocity upon impact with the bridge model. The pile foundations were fixed to the steel plates in the ground trough using clamps and further secured with bolts, as illustrated in Figure 3.

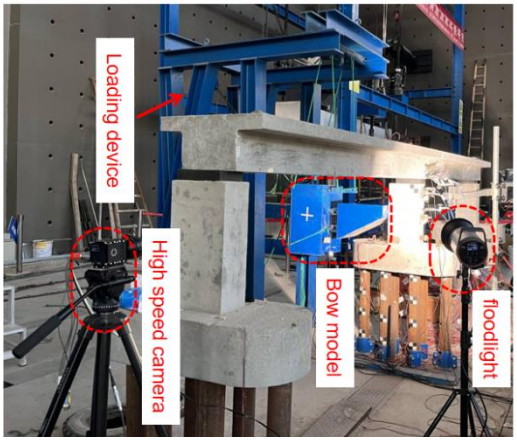


Figure 3 Scaled bridge collision test.

The ship-bridge collision process involves complex elastoplastic deformation of the bow. As the velocity increases, the deformation of the bow becomes more significant. This study conducted collision tests at two different heights, with impact points located 250 mm and 350 mm above the base of the pier, respectively. Analyzing the time-history curves of impact forces under different impact velocities at these two heights reveals that the change in impact location has almost no influence on the impact force. This is because the magnitude of the impact force is primarily determined by the contact area, and the change in impact location does not affect the contact area, as illustrated in Figure 4. Moreover, when the impact velocity exceeds 1.5 m/s, the peak impact force increases very slowly with further increases in velocity. This phenomenon is mainly attributed to the internal structure of the barge bow. Additionally, the stiffness of the barge bow is relatively high compared to other types of bows, resulting in the maximum impact force being reached almost immediately at the onset of collision.

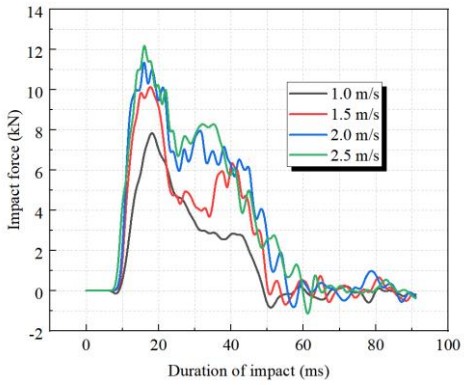


(a) 250 mm

DOI: 10.3217/978-3-99161-057-1-176

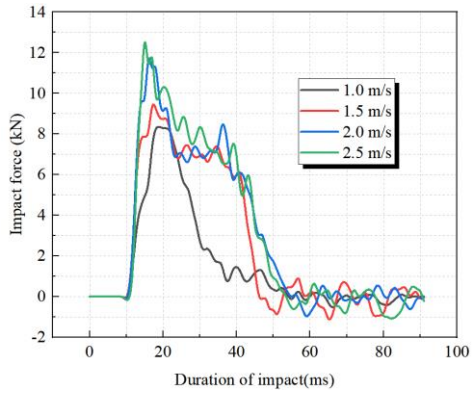


(b)350 mm

Figure 4. Time-history curve of ship-bridge collision force

After being subjected to impact, fine cracks appeared at the base of the pier. The cracks generated under the most critical impact condition are shown in Figure 5. At this stage, the cracks have not yet penetrated the entire cross-section of the pier, and their widths remain very small. Additionally, the strain values at the base of the pier caused by impacts at two different heights with a velocity of 2.5 m/s were recorded, as presented in Table 1.

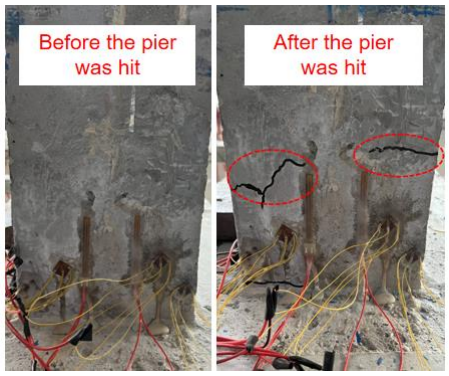


Figure 5. Comparative analysis of damage at the base of bridge piers

When the impact velocity is the same, a higher impact height results in greater strain. Larger strains are more likely to induce cracks at the base of the pier, indicating that a higher impact location increases the likelihood of damage to the pier base.

Table 1. Strain data at the base of bridge piers

| Impact velocity (m/s) | Height of impact (250 mm) | Height of impact (350 mm) |
|---|---|---|
| 2.5 | 113 | 171 |

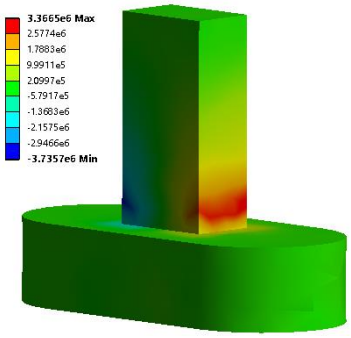


(a) 250 mm

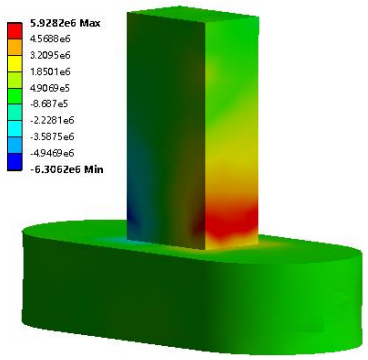


(b) 350 mm

Figure 6. Stress simulation at the base of bridge piers

A finite element model corresponding to the experimental model was established, and the stresses at the base of the pier under two impact heights with a velocity of 2.5 m/s were calculated, as shown in Figure 6. The strain values obtained from the experiments were converted into stress values, and the results showed minimal discrepancies compared to the finite element results. This indicates that the finite element modeling approach in this study aligns well with the actual conditions. When the stress at the base of the pier exceeds the tensile strength of the concrete, cracks begin to form. As the stress at the base gradually increases, the cracks progressively penetrate the entire cross-section of the pier. According to the Chinese building industry standard Code for Design of Concrete Structures (GB 50010-2010), the standard tensile strength of reinforced concrete can be calculated. When the stress at the base exceeds the standard tensile strength of reinforced concrete, it indicates that the pier has suffered severe damage.

## 3 DAMAGE CLASSIFICATION THEORY

The Box-Behnken Design (BBD) method was employed for sampling value calculations. Taking a three-factor design as an example, the distribution of sampling points is illustrated in Figure 7. Here, E represents the kinetic energy during ship impact, h denotes the impact height, and fc indicates the concrete strength grade. Subsequently, an actual ship-bridge collision model was established, and sampling value calculations were performed using the Box-Behnken Design. The obtained data were fitted to a surface, yielding the stress data at the base of the pier under the influence of the three factors in ship-bridge collisions.

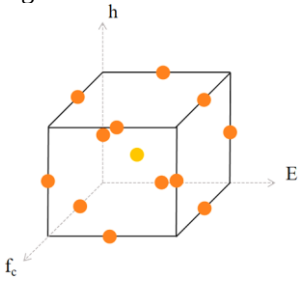


Figure 7. Sampling points for Box-Behnken Design

In the bridge ship collision fragility analysis studied in this paper, parameter A is defined as the impact kinetic energy of the ship. Specifically, the ship collision fragility is defined as the conditional failure probability that the structure reaches or exceeds a certain limit state (Ls) when subjected to a ship

DOI: 10.3217/978-3-99161-057-1-176

collision with impact kinetic energy A equal to E, as shown in Equation (1).

$$F_R(a) = P\left[Ls \middle| A = E\right] \tag{1}$$

The polynomial response surface surrogate model is a commonly used form of surrogate model in response surface analysis. In this study, a polynomial surrogate model is employed to fit the stress at the base of the pier caused by barge impact. The impact force generated by the barge collision increases with the kinetic energy of the ship. However, when the kinetic energy exceeds a certain threshold, the growth of the impact force slows down. Consequently, the tensile stress at the base of the pier follows the same trend, necessitating a segmented calculation approach for the tensile stress. Here, σt represents the tensile stress at the base of the pier, E0 denotes the critical segmentation point of kinetic energy, and EC represents the maximum kinetic energy used in the calculations.

$$\begin{aligned}\sigma_t = {} & p_1 + p_2 f_c + p_3 h + p_4 E + p_5 f_c h + \\ & p_6 f_c E + p_7 h E + p_8 f_c^2 + p_9 h^2 + p_{10} E^2\end{aligned} \tag{2}$$

$$\sigma_t = \begin{cases} \sigma_1\left(f_c, h, E\right), E \in \left(0, E_0\right) \\ \sigma_2\left(f_c, h, E\right), E \in \left(E_0, E_c\right) \end{cases} \tag{3}$$

The fragility curve of the pier is obtained by performing Monte Carlo sampling on the normally distributed random variable fc and plotting the failure probabilities corresponding to different kinetic energies, thereby generating the fragility curve. The probability distribution of C30 concrete strength is shown in Table 2.

Table 2 Distribution of concrete strength grades

| Concrete strength | Nominal value | Mean value | Coefficient of variation (%) |
|---|---|---|---|
| $f_c$ | 30 MPa | 30 MPa | 15 |

## 4 FAILURE PROBABILITY CALCULATION

A finite element model of the actual bridge was established, with the pier having a width of 3 m, a length of 6.5 m, and a height of 20 m. The hull was modeled using the AASHTO barge model. A comparison of the impact force and the tensile stress at the pier base under different ship kinetic energies reveals that the trends of change in impact force and tensile stress are remarkably similar. Furthermore, the installation of collision protection devices was considered to further verify whether the trends of change in impact force and tensile stress remain consistent.

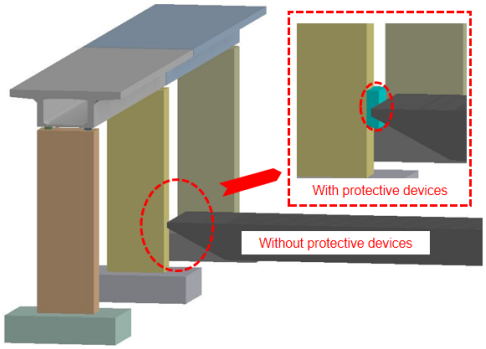


Figure 8. Full size bridge collision model

The results indicate that the trends of change in the impact force caused by ship-bridge collisions and the tensile stress generated at the pier base are consistent. Even with the addition of protective devices, this regularity remains unaffected. Therefore, the trend of change in barge impact force with respect to ship kinetic energy can be used to describe the trend of change in tensile stress with respect to ship kinetic energy. Moreover, both the peak impact force and the peak tensile stress increase with the rise in ship kinetic energy, but the trend of change exhibits a segmented pattern. When the ship's kinetic energy is below a critical threshold, the trends of change in impact force and tensile stress are rapid. Once the ship's kinetic energy exceeds the critical value, the trends of change in impact force and tensile stress become more gradual, as illustrated in Figure 9.

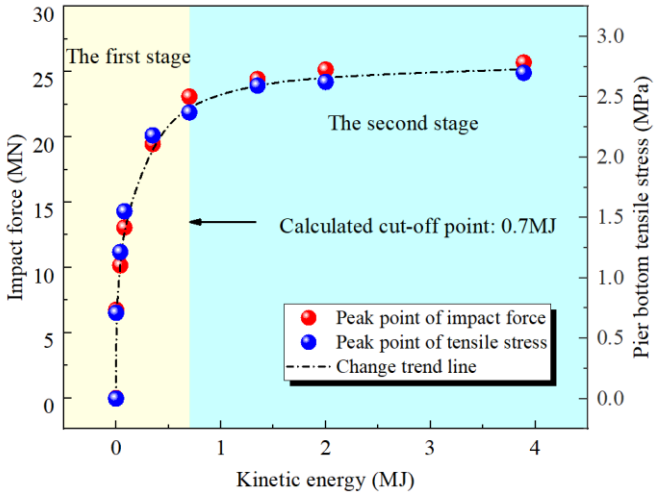


(a) Without protective devices

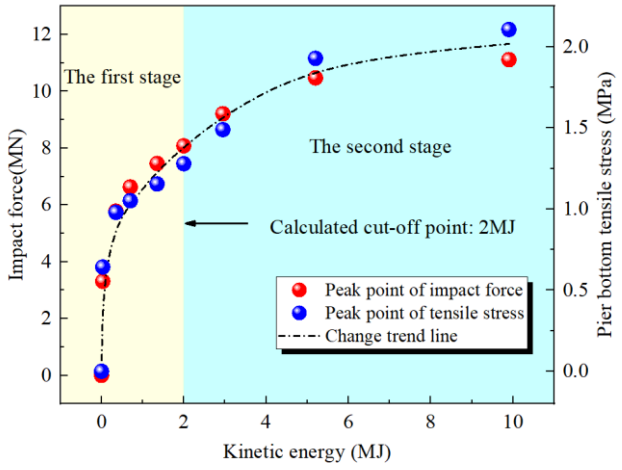


(b) With protective devices

Figure 9. The trend of impact force-tensile stress variation

According to the calculated results, it can be determined that the kinetic energy segmentation point for ship-bridge collisions without protective devices is 0.7 MJ. According to the sampling method of Box-Behnken Design, the tensile stresses at the base of the pier under different influencing factors were obtained through finite element calculations, as shown in Table 3.

The obtained tensile stresses at the base of the pier under different influencing factors were fitted to a surface, yielding the values of the undetermined coefficients for the two segments, as shown in Table 4.

DOI: 10.3217/978-3-99161-057-1-176

Table 3. Sampling values for numerical simulation

| Concrete strength (MPa) | Height of impact (m) | Kinetic energy (MJ) | Pier bottom tensile stress (MPa) | Kinetic energy (MJ) | Pier bottom tensile stress (MPa) |
|---|---|---|---|---|---|
| 20 | 3 | 0.35 | 1.303 | 1.35 | 1.468 |
| 40 | 3 | 0.35 | 1.441 | 1.35 | 1.806 |
| 20 | 9 | 0.35 | 2.299 | 1.35 | 2.678 |
| 40 | 9 | 0.35 | 2.607 | 1.35 | 3.104 |
| 20 | 6 | 0 | 0 | 0.7 | 2.178 |
| 40 | 6 | 0 | 0 | 0.7 | 2.587 |
| 20 | 6 | 0.7 | 2.178 | 2.0 | 2.457 |
| 40 | 6 | 0.7 | 2.587 | 2.0 | 2.864 |
| 30 | 3 | 0 | 0 | 0.7 | 1.466 |
| 30 | 9 | 0 | 0 | 0.7 | 2.798 |
| 30 | 3 | 0.7 | 1.466 | 2.0 | 1.808 |
| 30 | 9 | 0.7 | 2.798 | 2.0 | 3.022 |
| 30 | 6 | 0.35 | 2.181 | 1.35 | 2.593 |
| 30 | 6 | 0.35 | 2.185 | 1.35 | 2.598 |
| 30 | 6 | 0.35 | 2.178 | 1.35 | 2.587 |
| 30 | 6 | 0.35 | 2.182 | 1.35 | 2.588 |
| 30 | 6 | 0.35 | 2.184 | 1.35 | 2.592 |

The obtained tensile stresses at the base of the pier under different influencing factors were fitted to a surface, yielding the values of the undetermined coefficients for the two segments, as shown in Table 4.

Table 4 Sampling values for undetermined parameters

| Coefficient value | $E<E_0$ | $E \geqslant E_0$ |
|---|---|---|
| $P_1$ | -0.6629 | -1.1001 |
| $P_2$ | 0.0266 | 0.0385 |
| $P_3$ | 0.2600 | 0.5611 |
| $P_4$ | 3.0525 | 0.6283 |
| $P_5$ | 0.0017 | 0.0011 |
| $P_6$ | 0.0143 | 0.0016 |
| $P_7$ | 0.1978 | 0.0032 |
| $P_8$ | -0.0005 | -0.0005 |
| $P_9$ | -0.0187 | -0.0326 |
| $P_{10}$ | -3.7999 | -0.1819 |

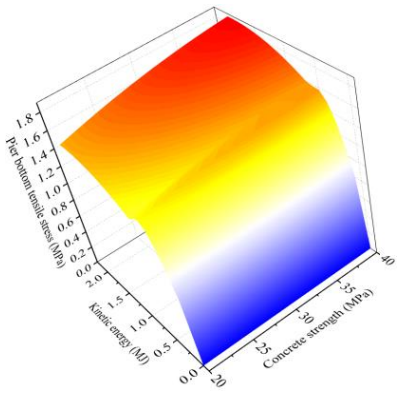


(a) The impact height was 3 m

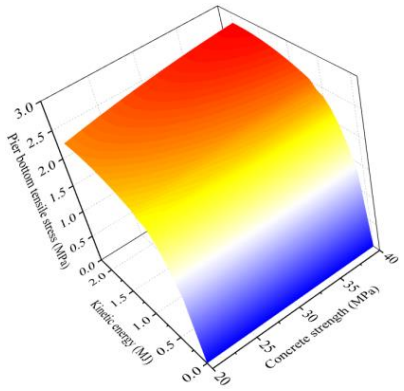


(b) The impact height was 6 m

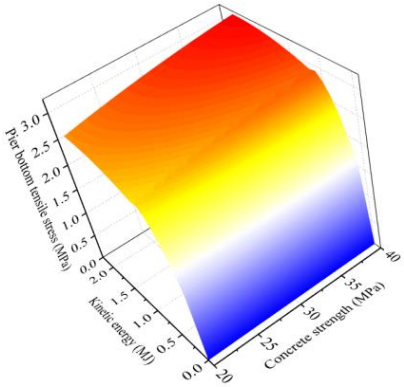


(c) The impact height was 9 m

Figure 10. The combined effect of kinetic energy and concrete strength

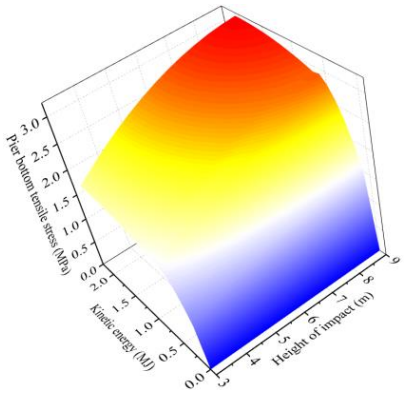


(a) The concrete strength is C20

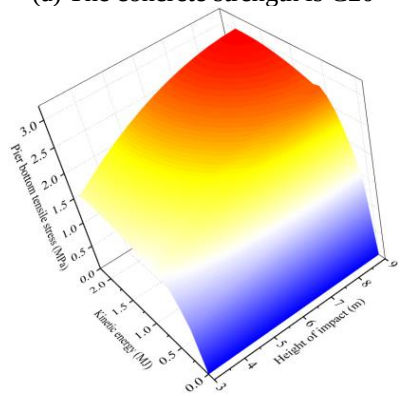


(b) The concrete strength is C30

DOI: 10.3217/978-3-99161-057-1-176

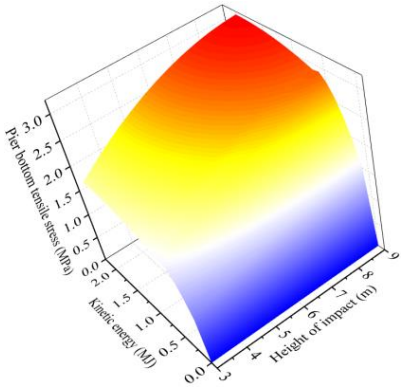


(c) The concrete strength is C40

Figure 11. The combined effect of kinetic energy and impact height

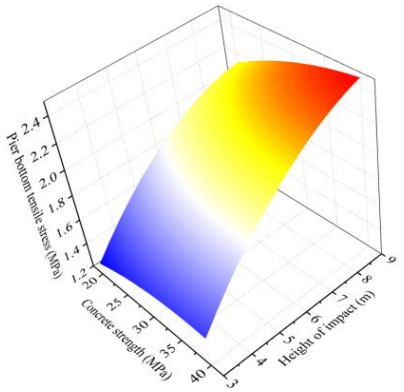


(a) The impact kinetic energy is 0.35 MJ

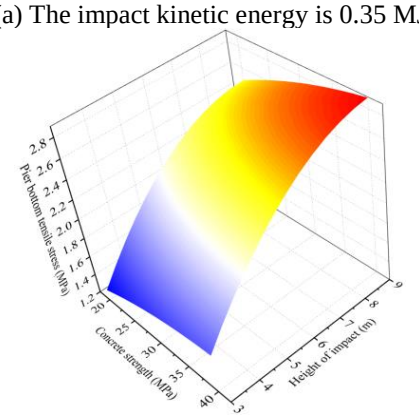


(b) The impact kinetic energy is 0.7 MJ

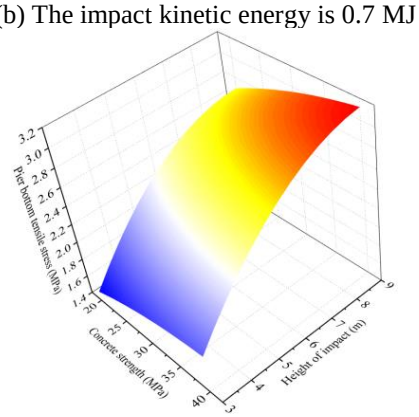


(c) The impact kinetic energy is 1.35 MJ

Figure 12. The combined effect of concrete strength and impact height

The impact height and impact kinetic energy have a significant influence on the tensile stress at the pier base, whereas the concrete strength has a relatively minor effect on the tensile stress at the pier base. Therefore, in the subsequent vulnerability calculations, the primary considerations will be the effects of impact kinetic energy and impact height.

The fragility curves of the pier under three impact height conditions were obtained through Monte Carlo sampling, as shown in Figure 13. Since the tensile strength of C30 concrete is 2.01 MPa, the condition where the tensile stress at the base of the pier exceeds 2.01 MPa is considered as the onset of minor failure, the initiation of cracks in the pier.

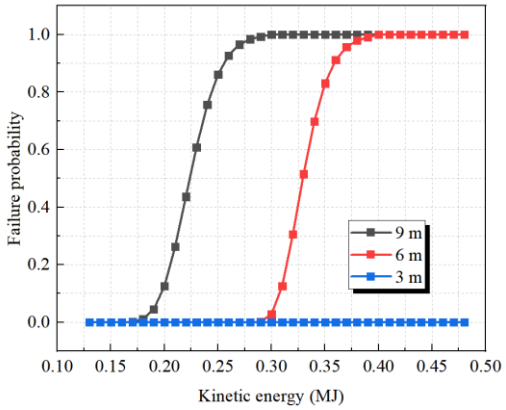


Figure 13. Fragility curves for different impact heights

As the tensile stress at the base caused by the impact does not reach the standard tensile strength of reinforced concrete, only minor failure conditions of the pier need to be considered. For the impact height of 9 m, there is a probability of minor failure when the barge's kinetic energy reaches 0.18 MJ, and direct failure occurs when the kinetic energy exceeds 0.3 MJ. For the impact height of 6 m, minor failure begins to occur when the barge's kinetic energy reaches 0.3 MJ, and direct failure occurs when the kinetic energy exceeds 0.4 MJ. For the impact height of 3 m, failure is almost negligible.

## 5 CONCLUSIONS

In this study, the magnitude of tensile stress at the base of the pier caused by barge impact is used as the damage assessment indicator. A fragility analysis method for bridge ship collisions based on the response surface method is proposed. This method enables rapid fragility assessment of the pier when subjected to barge impact.

The established high-precision response surface model can replace structural models that require complex nonlinear calculations. The developed response surface surrogate model can be utilized for extensive sample analysis in bridge ship collision fragility studies. When subjected to barge impact, the trend of tensile stress at the base of the pier is closely related to the critical barge kinetic energy, exhibiting a segmented characteristic similar to the impact force. Therefore, to accurately reflect the true response characteristics of the pier under barge impact, the sample design should be segmented based on the critical barge kinetic energy. Through a comparative analysis of the individual effects of the three factors on the fragility of the pier, it is evident that the magnitude of tensile stress at the base of the pier is significantly influenced by the impact height and impact kinetic energy,

DOI: 10.3217/978-3-99161-057-1-176

while changes in concrete grade have a relatively minor effect on the tensile stress. However, the higher the concrete strength grade, the greater the standard tensile strength of the pier, enhancing its resistance to impact and reducing the likelihood of severe damage.

## ACKNOWLEDGMENTS

Funding: This work was supported by the National Key R&D Program of China [Grant Numbers. 2024YFC3015200], and National Natural Science Foundation of China [Grant Numbers. U1709207].

## REFERENCES

[1] Chen, T. L., Wu, H., & Fang, Q. (2022). Impact force models for bridge under barge collisions. Ocean Eng, 259, 111856.
[2] Nian, Y., Wan, S., Wang, X., Zhou, P., Avcar, M., & Li, M. (2023). Study on crashworthiness of nature-inspired functionally graded lattice metamaterials for bridge pier protection against ship collision. Eng Struct, 277, 115404.
[3] Song, S., Xie, Y., Wang, Y., Zhang, W., Kurtulus, A., Apaydin, N. M., & Taciroglu, E. (2024). Seismic fragility and vulnerability assessment of a multi-span irregular curved bridge under spatially varying ground motions. Soil Dyn Earthq Eng, 180, 108585.
[4] Wang, L., Che, J., Dou, C., Li, X., Zhu, Y., Wang, R., & Wu, T. (2025). Seismic vulnerability evolution of large cantilever cap bridges due to material degradation. Structures, 72, 108303.
[5] Li, Y., Chen, H., Yi, M., Li, J., & Fang, C. (2025). Seismic vulnerability analysis of bridges incorporating scour uncertainty using a copula-based approach. Ocean Eng, 323, 120598.
[6] Kameshwar, S., & Padgett, J. E. (2018). Response and fragility assessment of bridge columns subjected to barge-bridge collision and scour. Eng Struct, 168, 308-319.
[7] Fu, J., Wang, W., Wang, X., Zhao, W., Zhou, R., & Lu, Z. (2024). Fragility assessment of RC bridge piers subjected to vehicle collision based on residual load-bearing capacity. Structures, 68, 107103.
[8] Zhong, Z., Fan, W., Liu, B., Huang, X., & Geng, B. (2024). A fragility-based framework for identification of unfavorable impact location for bridge columns under barge collisions. Ocean Eng, 294, 116839.
[9] Fan, W., Sun, Y., Shen, D. J., & Liu, b. (2021). Vessel-collision vulnerability analysis method of bridge structures based on simplified model with girders and response surface. J Hunan Univ, 48(03), 34-43.
[10] Fan, W., Xu, X., Zhang, Z., & Shao, X. (2018). Performance and sensitivity analysis of UHPFRC-strengthened bridge columns subjected to vehicle collisions. Eng Struct, 173, 251-268.
[11] Duan, X., Zhang, J., Liu, L., Hu, J., & Xue, Y. (2024). Hybrid response surface method for system reliability analysis of pile-reinforced slopes. J Rock Mech Geotech Eng, 16(9), 3395-3406..